



Positive matrix
factorization of PM_{2.5}

M. Xie et al.

Positive matrix factorization of PM_{2.5} – eliminating the effects of gas/particle partitioning of semivolatile organic compounds

M. Xie¹, K. C. Barsanti², M. P. Hannigan¹, S. J. Dutton³, and S. Vedal⁴

¹Department of Mechanical Engineering, College of Engineering and Applied Science,
University of Colorado, Boulder, CO 80309, USA

²Department of Civil and Environmental Engineering, Portland State University, P.O. Box 751,
Portland, OR 97207, USA

³National Center for Environmental Assessment, US Environmental Protection Agency,
Research Triangle Park, NC 27711, USA

⁴Department of Environmental and Occupational Health Sciences, School of Public Health,
University of Washington, Seattle, WA 98195, USA

Title Page

Abstract

Introduction

Conclusions

References

Tables

Figures

⏪

⏩

◀

▶

Back

Close

Full Screen / Esc

Printer-friendly Version

Interactive Discussion



Received: 3 January 2013 – Accepted: 9 February 2013 – Published: 22 February 2013

Correspondence to: M. Xie (mingjie.xie@colorado.edu) and
M. P. Hannigan (hannigan@colorado.edu)

Published by Copernicus Publications on behalf of the European Geosciences Union.

ACPD

13, 5199–5232, 2013

Positive matrix factorization of $PM_{2.5}$

M. Xie et al.

Title Page

Abstract

Introduction

Conclusions

References

Tables

Figures

⏪

⏩

◀

▶

Back

Close

Full Screen / Esc

Printer-friendly Version

Interactive Discussion



Abstract

Gas-phase concentrations of semi-volatile organic compounds (SVOCs) were calculated from gas/particle (G/P) partitioning theory using their measured particle-phase concentrations. The particle-phase data were obtained from an existing filter measurement campaign (27 January 2003–2 October 2005) as a part of the Denver Aerosol Sources and Health (DASH) study, including 970 observations of 71 SVOCs (Xie et al., 2013). In each compound class of SVOCs, the lighter species (e.g. docosane in *n*-alkanes, fluoranthene in PAHs) had higher total concentrations (gas + particle phase) and lower particle-phase fractions. The total SVOC concentrations were analyzed using positive matrix factorization (PMF). Then the results were compared with source apportionment results where only particle-phase SVOC concentrations were used (filter-based study; Xie et al., 2013). For the filter-based PMF analysis, the factors primarily associated with primary or secondary sources (*n*-alkane, EC/sterane and inorganic ion factors) exhibit similar contribution time series ($r = 0.92$ – 0.98) with their corresponding factors (*n*-alkane, sterane and nitrate + sulfate factors) in the current work. Three other factors (light *n*-alkane/PAH, PAH and summer/odd *n*-alkane factors) are linked with pollution sources influenced by atmospheric processes (e.g. G/P partitioning, photochemical reaction), and were less correlated ($r = 0.69$ – 0.84) with their corresponding factors (light SVOC, PAH and bulk carbon factors) in the current work, suggesting that the source apportionment results derived from filter-based SVOC data could be affected by atmospheric processes. PMF analysis was also performed on three temperature-stratified subsets of the total SVOC data, representing ambient sampling during cold (daily average temperature $< 10^{\circ}\text{C}$), warm ($\geq 10^{\circ}\text{C}$ and $\leq 20^{\circ}\text{C}$) and hot ($> 20^{\circ}\text{C}$) periods. Unlike the filter-based study, in this work the factor characterized by the low molecular weight (MW) compounds (light SVOC factor) exhibited strong correlations ($r = 0.82$ – 0.98) between the full data set and each sub-data set solution, indicating that the impacts of G/P partitioning on receptor-based source apportionment could be eliminated by using total SVOC concentrations.

Positive matrix factorization of $\text{PM}_{2.5}$

M. Xie et al.

Title Page

Abstract

Introduction

Conclusions

References

Tables

Figures

◀

▶

◀

▶

Back

Close

Full Screen / Esc

Printer-friendly Version

Interactive Discussion



1 Introduction

The Denver Aerosol Sources and Health (DASH) study was designed to explore the associations between short-term exposure to individual $PM_{2.5}$ components, sources and negative health effects (Vedal et al., 2009). Daily 24-h $PM_{2.5}$ sampling was conducted from mid-2002 to the end of 2008. Speciation of $PM_{2.5}$ has been carried out for gravimetric mass, inorganic ionic compounds (sulfate, nitrate and ammonium) and carbonaceous components, including elemental carbon (EC), organic carbon (OC) and a large array of semi-volatile organic compounds (SVOCs). Kim et al. (2012) have investigated the lag structure of the association between $PM_{2.5}$ constituents and hospital admissions by disease using the 5-yr bulk speciation data set of DASH study (nitrate, sulfate, EC and OC). They found that the estimated short-term effects of $PM_{2.5}$ bulk components, especially those of EC and OC, were more immediate for cardiovascular diseases and more delayed for respiratory diseases. Future work will focus on the association between specific $PM_{2.5}$ sources and health outcomes.

To develop control strategies for $PM_{2.5}$, receptor-based models (e.g. positive matrix factorization, chemical mass balance) have been applied to quantitatively apportion $PM_{2.5}$ to sources that are detrimental to human health (Laden et al., 2000; Mar et al., 2005; Ito et al., 2006). One basic assumption of receptor-based models is that source profiles are constant over the period of ambient and source sampling (Chen et al., 2011). However, the output factors of a receptor model are not necessarily emission sources, and could be affected by atmospheric processes like photochemical reaction or gas/particle (G/P) partitioning (May et al., 2012). The influence of atmospheric processes on certain output factors can change with meteorological conditions (e.g. solar irradiance, ambient temperature). Thus, the assumption of constant source profiles does not hold for all output factors, especially for long time series studies.

$PM_{2.5}$ associated SVOCs data have been used as inputs for receptor models in many studies (Jaeckels et al., 2007; Schnelle-Kreis et al., 2007; Shrivastava et al., 2007; Dutton et al., 2010). All SVOCs are subject to G/P partitioning and thus partly

ACPD

13, 5199–5232, 2013

Positive matrix factorization of $PM_{2.5}$

M. Xie et al.

Title Page

Abstract

Introduction

Conclusions

References

Tables

Figures

◀

▶

◀

▶

Back

Close

Full Screen / Esc

Printer-friendly Version

Interactive Discussion



distributed in the gas phase. According to the G/P partitioning theory developed by Pankow (1994a, b), which has been applied to the predictions of particulate matter (PM) formation (Liang and Pankow, 1996; Liang et al., 1997; Mader and Pankow, 2002), the partitioning of each individual compound is governed by its absorptive G/P partitioning coefficient, $K_{p,OM}$, which can either be measured directly (Eq. 1) or calculated from theory (Eq. 2):

$$K_{p,OM} = \frac{K_p}{f_{OM}} = \frac{F/M_{OM}}{A} \quad (1)$$

$$K_{p,OM} = \frac{RT}{10^6 \overline{MW}_{OM} \zeta_{OM} \rho_L^0} \quad (2)$$

where it is assumed that particle-phase organic material (OM) is primarily responsible for the absorptive uptake. Thus, it is meaningful to normalize the G/P partitioning constant (K_p , $m^3 \mu g^{-1}$) by the weight fraction of the absorptive OM phase (f_{OM}) in the total PM phase (Eq. 1), so as to obtain $K_{p,OM}$ ($m^3 \mu g^{-1}$). F ($ng m^{-3}$) is the mass concentration of each compound associated with the particle phase; A ($ng m^{-3}$) is the mass concentration of each compound in the gas phase; M_{OM} ($\mu g m^{-3}$) is the mass concentration of the particle-phase OM; R ($m^3 atm K^{-1} mol^{-1}$) is the ideal gas constant; T (K) is the ambient temperature; \overline{MW}_{OM} ($g mol^{-1}$) is the mean molecular weight (MW) of the absorbing OM phase; ζ_{OM} is the mole fraction scale activity coefficient of each compound in the absorbing OM phase; and ρ_L^0 (atm) is the vapor pressure of each pure compound. For a given SVOC and a single OM phase, the G/P partitioning is only controlled by ambient temperature (Eq. 2). The mass fraction of the total SVOC in the atmosphere that contributes to the particle phase thus can change with ambient temperature. As such, the source profiles of particle-phase SVOCs are expected to vary due to the influence of G/P partitioning, especially for those sources primarily contributing light SVOCs (e.g. docosane, fluoranthene). Therefore, when using a long time series of speciated $PM_{2.5}$ data as input for receptor model analysis, the light SVOC

Positive matrix factorization of $PM_{2.5}$

M. Xie et al.

Title Page

Abstract

Introduction

Conclusions

References

Tables

Figures

◀

▶

◀

▶

Back

Close

Full Screen / Esc

Printer-friendly Version

Interactive Discussion



related sources/factors for a sub period of observation might be obscured by the influence of G/P partitioning, which will subsequently affect the health effect estimation of specific PM_{2.5} sources.

In this study, gas-phase SVOC concentrations were estimated using their particle-phase concentrations based on Eq. (1). The particle-phase concentrations of SVOCs were obtained from an existing 32-month series of daily PM_{2.5} speciation, which has been used for source apportionment in a previous study (Xie et al., 2013). In order to eliminate the influence of G/P partitioning on source apportionment, the total concentrations of gas- and particle-phase SVOCs were used as inputs for PMF analysis. The PMF2 model (Paatero, 1998a,b), coupled with a stationary block bootstrap technique quantifying errors due to random sampling (Hemann et al., 2009), was the primary source apportionment tool. Moreover, the 32-month data set of total SVOCs was divided into three sub-data sets by daily average temperature for source apportionment using the identical method. The use of smaller sub-data sets as inputs is to verify the elimination of G/P partitioning influence from the total SVOC-based PMF analysis.

2 Methods

2.1 Particle phase measurements

Daily PM_{2.5} samples were collected on the top of a two-story elementary school building in urban Denver. Details of the sampling site, set up, protocols and chemical analysis have been published by Vedal et al. (2009) and Dutton et al. (2009a,b). Daily average particle-phase SVOCs concentrations were obtained from existing PM_{2.5} measurements, including 970 observations of 71 species (27 January 2003–2 October 2005). Concentrations of inorganic ions, bulk elemental carbon (EC) and organic carbon (OC) were also measured for the same study period. The pointwise, blank corrected concentration uncertainties of each species were estimated by using the root sum of squares (RSS) method (Dutton et al., 2009a,b). The concentration and uncertainty data sets

Positive matrix factorization of PM_{2.5}

M. Xie et al.

Title Page

Abstract

Introduction

Conclusions

References

Tables

Figures

◀

▶

◀

▶

Back

Close

Full Screen / Esc

Printer-friendly Version

Interactive Discussion



have been used as inputs for a filter-based source apportionment in a previous study (Xie et al., 2013). The meteorological (temperature, relative humidity and solar irradiance) and trace gas (ozone, nitrogen oxides (NO_x) and CO) data used in this study were also obtained from Xie et al. (2013).

2.2 Gas phase concentration and uncertainty estimation

The $K_{p,OM}$ value for each species on each day was calculated by Eq. (2). Here four parameters are required, including T , \overline{MW}_{OM} , ζ_{OM} and p_L^0 . For this application T is the measured daily average temperature. Based on smog chamber and ambient studies (Odum et al., 1996; Hallquist et al., 2009), 150–250 g mol⁻¹ is a reasonable range for the average MW of the particulate OM phase; here we assume the \overline{MW}_{OM} to be 200 g mol⁻¹ for all samples, as is used in previous work (Barsanti and Pankow, 2004; Williams et al., 2010). Values of ζ_{OM} were assumed to be unity for all species in each sample. Values of p_L^0 were estimated using the group contribution methods (GCMs) SPARC (Hilal et al., 1995; <http://archemcalc.com/sparc/test/>) and SIMPOL (Pankow and Asher, 2008). The p_L^0 value for each species on each day was adjusted by daily average temperature:

$$p_L^0 = p_L^{0,*} \exp \left[\frac{\Delta H_{vap}^*}{R} \left(\frac{1}{298.15} - \frac{1}{T} \right) \right] \quad (3)$$

where $p_L^{0,*}$ is the vapor pressure of each pure compound at 298.15 K; ΔH_{vap}^* is the enthalpy of vaporization of the liquid (kJ mol⁻¹) at 298.15 K. The $p_L^{0,*}$, ΔH_{vap}^* and average $K_{p,OM}$ value for each species are given in Table S1.

Gas-phase concentrations of each SVOC were calculated by Eq. (1). The values of F for each SVOC in Eq. (1) were obtained from existing PM_{2.5} measurements (Xie et al., 2013); M_{OM} was estimated by multiplying the OC concentrations by a scaling factor of 1.53, which resulted in optimum mass closure of PM_{2.5} in a previous DASH

Title Page

Abstract

Introduction

Conclusions

References

Tables

Figures

◀

▶

◀

▶

Back

Close

Full Screen / Esc

Printer-friendly Version

Interactive Discussion



study (Dutton et al., 2009a). The total concentration of each SVOC (S , gas + particle phase) on each day is then obtained by Eq. (4),

$$S = F + A = \frac{1 + K_{p,OM}M_{OM}}{K_{p,OM}M_{OM}} F \quad (4)$$

The uncertainty associated with S estimation was also calculated using the RSS method,

$$\delta S = \sqrt{\left(\frac{\partial S}{\partial F} \delta F\right)^2 + \left(\frac{\partial S}{\partial M_{OM}} \delta M_{OM}\right)^2} \quad (5)$$

where δS is the propagated uncertainty in S ; δF and δM_{OM} are the propagated uncertainties associated with particle-phase SVOC and M_{OM} measurements, and could be obtained from the uncertainty data sets introduced in Sect. 2.1. The $K_{p,OM}$ value uncertainty was not estimated in the current work. Statistics for the total concentration of each SVOC from 27 January 2003 to 2 October 2005 are listed in Table S1, including the mean and median concentrations, mean particle-phase fractions, signal to noise ratios ($S/N = \text{mean concentration}/\text{mean uncertainty}$) and coefficients of variation ($CV = \text{standard deviation}/\text{mean concentration}$). Table S1 also lists statistics of particulate bulk components (mass, nitrate, sulfate, ammonium, EC and OC). The OC concentrations are shown in 5 fractions (OC1–4 and PC), representing the carbon measured at four distinct temperature steps (340, 500, 615 and 900 °C) with a pyrolyzed carbon adjustment in the first heating cycle of NOISH 5040 thermal optical transmission (TOT) method (NOISH, 2003; Schauer et al., 2003).

2.3 PMF analysis and uncertainty assessment

PMF2 (Paatero, 1998a,b), a multivariate receptor model, was used for source apportionment in this study. It is the primary source apportionment tool applied in the DASH

Title Page

Abstract

Introduction

Conclusions

References

Tables

Figures

◀

▶

◀

▶

Back

Close

Full Screen / Esc

Printer-friendly Version

Interactive Discussion



Positive matrix factorization of PM_{2.5}

M. Xie et al.

Title Page

Abstract

Introduction

Conclusions

References

Tables

Figures

◀

▶

◀

▶

Back

Close

Full Screen / Esc

Printer-friendly Version

Interactive Discussion



project, and is discussed in detail by Dutton et al. (2010). PMF uses an uncertainty-weighted least-squares fitting approach to identify distinct factor profiles and quantify factor contributions from a time series of observations. The bias and variability in factor profile and contribution due to random sampling error were estimated by applying a method from Hemann et al. (2009). 1000 replicate data sets were generated from the original data set using a stationary block bootstrap technique and each was analyzed with PMF. Because the ordering of factors may differ across solutions on bootstrap replicate data sets (e.g. factor i in one solution may correspond to factor j in another), the Multilayer Feed Forward Neural Networks were trained to sort and align the factor profiles from each PMF bootstrap solution to that of the original solution based on the observed data (known as the base case). A PMF bootstrap solution was recorded only when each factor of that solution could be uniquely matched to a base case factor. The measurement days resampled in each recorded solution were tracked to examine the bias and variability in contribution of each factor on each day, which could then be used to assess the variability of the PMF model fit. In this work, the factor number was determined based on the interpretability of different PMF solutions (5–9 factors) as well stability across bootstrap-replicate data sets as represented by factor matching rate.

2.4 Preparation of PMF input data set

Fifty one SVOCs and four bulk species were selected from all species with 970 daily observations for filter-based PM_{2.5} source apportionment (Xie et al., 2013). The species screening was based on the percentage of missing values and observations below detection limit (BDL), S/N ratios and the stability of PMF solution. In this work, the candidate SVOCs for source apportionment were selected from the fifty one species used in the previous study. Bulk species were selected from nitrate, sulfate, EC and the five OC fractions. Interpretability and factor matching rate ($> 50\%$) of the PMF solution were criteria for species screening. Among the five OC fractions, the OC1 concentration was measured under the lowest temperature (340 °C) and most likely influenced by G/P partitioning; and the gas-phase concentration of OC1 could not be estimated

due to the complex composition. The OC4 concentration was very low with low *S/N* ratio. Thus OC1 and OC4 were excluded for PMF analysis. The other three fractions (OC2, OC3, PC) were assumed to be less or non-volatile and were included for PMF analysis. Finally, the six bulk species with 970 daily observations and forty six SVOCs with 970 estimated total concentrations constituted the primary PMF input data set.

Similarly to the previous Xie et al. (2013) study, PMF analysis was also performed for three temperature-stratified subsets of the original 970 samples. The three sub-data sets consisted of sampling days with daily average temperature less than 10 °C (*N* = 364), between 10 °C and 20 °C (*N* = 318), and greater than 20 °C (*N* = 288), respectively. The sampling periods of these three sub-data sets were defined as cold, warm and hot. The statistics of total SVOCs during each of these three periods are shown in Tables S2–S4. PMF input species screening for each sub-data set was conducted in the same manner as for the full data set.

3 Result and discussion

3.1 Total SVOCs and their particle-phase fractions

Except steranes, the low MW species have the highest total concentrations and the lowest particle-phase fractions in each class of SVOCs (Table S1). For example, docosane and fluoranthene are the most abundant species in *n*-alkanes and PAHs with mean concentrations of 32.8 ngm⁻³ and 11.2 ngm⁻³ respectively, one to two orders of magnitudes higher than those of high MW species in their chemical classes. In this study, the total concentrations of light *n*-alkane (e.g. docosane–pentacosane) and PAH (e.g. MW = 202) species increased by more than 100 % from the cold to the hot periods (Tables S2–S4), possibly due to the evaporation of fossil fuels (Nahir, 1999) and increases in biogenic VOC emissions with increasing temperature.

The average particle-phase fraction of each SVOC was calculated for the cold, warm and hot periods and shown in Fig. 1. All SVOCs exhibit the highest particle-phase

[Title Page](#)[Abstract](#)[Introduction](#)[Conclusions](#)[References](#)[Tables](#)[Figures](#)[◀](#)[▶](#)[◀](#)[▶](#)[Back](#)[Close](#)[Full Screen / Esc](#)[Printer-friendly Version](#)[Interactive Discussion](#)

Positive matrix factorization of PM_{2.5}

M. Xie et al.

Title Page

Abstract

Introduction

Conclusions

References

Tables

Figures

◀

▶

◀

▶

Back

Close

Full Screen / Esc

Printer-friendly Version

Interactive Discussion



fractions in cold periods and the lowest in hot periods, especially for those light SVOCs (e.g. docosane, fluoranthene), indicating a change in G/P partitioning behavior across different temperatures. Long chain *n*-alkanes (chain length > 27), heavy PAHs (MW > 252), steranes, hopanes, and sterols are mostly in the particle phase (> 75%) for all periods and less subject to evaporation (or partitioning to the gas phase) under higher temperatures. In Table S5, the estimated particle-phase fractions of selected SVOCs (*n*-alkanes, PAHs, sterane and hopanes) in hot periods are more comparable with those observed by Fraser et al. (1997, 1998) in summer Los Angeles than in summer Athens (Greece) (Mandalakis et al., 2002). Average fractions of particulate PAHs for the whole period are similar to those annual averages measured by Tsapakis and Stephanou (2005) in Heraklion (Greece). While large differences were observed for the particle-phase fractions of light PAHs (MW < 252) in cold and hot periods compared with those measured in urban Chicago (Simcik et al., 1997, 1998). These comparisons indicate that the estimations of G/P distributions of the SVOCs in this work are reasonable. Keep in mind that these differences may be influenced by parameters other than T , like MW_{OM} , ζ_{OM} and M_{OM} in Eqs. (1) and (2).

3.2 Sensitivity of total SVOC estimation based on G/P partitioning theory

Based on G/P partitioning theory, changes in ambient temperature lead to the evaporation or condensation of SVOCs; the extent of such changes with temperature depend in part on values of \overline{MW}_{OM} and ζ_{OM} , here assumed to be 200 g mol^{-1} and unity respectively. However, \overline{MW}_{OM} and ζ_{OM} are highly dependent on the composition of PM, which is complex in an urban area and mostly unknown. The \overline{MW}_{OM} values are typically based on MW of organic compounds detected in laboratory and field studies, but in some cases (e.g. under high relative humidity, RH) need to be adjusted downward for the presence of water in the particulate OM phase (Pankow and Chang, 2008; Chang and Pankow, 2010). The ζ_{OM} values for organic compounds in atmospheric applications are not necessarily unity for different SVOCs in varied PM composition (e.g.

varied amounts of polar and non-polar organic compounds and water) (Pankow and Chang, 2008; Pun, 2008). The uncertainties in these two parameters, as well as the OM/OC ratio, could affect the estimation of total SVOC concentration as described in Sect. 3.1.

5 Combining Eqs. (2) and (4), the equation for total SVOC calculation can be re-written as:

$$S = F + A = \left(1 + \frac{10^6 \rho_L^0 \overline{MW}_{OM} \zeta_{OM}}{RT M_{OM}} \right) F \quad (6)$$

from which we can infer that the estimation of total concentration (S value) for specific SVOC is primarily determined by the following term:

$$10 \quad z = \frac{10^6 \rho_L^0 \overline{MW}_{OM} \zeta_{OM}}{RT M_{OM}} \quad (7)$$

if z is close to 0, then most of the target SVOC is in particle phase; if z is close to or higher than 1, then the target SVOC is strongly subject to G/P partitioning. The sensitivity of total SVOC estimation (S value) to T , ζ_{OM} , OM/OC ratio, \overline{MW}_{OM} can be evaluated as the changes of z value to these uncertain parameters in Eq. (7). To test the sensitivity, the average temperatures and OC concentrations during the cold, warm
 15 and hot periods (defined in Sect. 2.4) were investigated; docosane was selected as an example to represent SVOCs with similar pure vapor pressure and G/P partitioning behavior. Three ζ_{OM} (0.5, 1.0, 1.5) and four \overline{MW}_{OM} (50, 150, 200, 300 g mol^{-1}) values, based on Pankow and Chang (2008) and four OM/OC (1.3, 1.4, 1.5, 1.6) ratios, based
 20 on Bae et al. (2006), were used to test the sensitivity of z value (or S value) calculation. The values of the above parameters investigated were listed in Table 1.

In Fig. 2, the sensitivity of z value to T , ζ_{OM} , OM/OC ratio and \overline{MW}_{OM} are shown in nine mesh plots. Each mesh plot exhibits the changes of z value to varied M_{OM} and

Positive matrix factorization of PM_{2.5}

M. Xie et al.

Title Page

Abstract

Introduction

Conclusions

References

Tables

Figures

◀

▶

◀

▶

Back

Close

Full Screen / Esc

Printer-friendly Version

Interactive Discussion



\overline{MW}_{OM} for a given T and ζ_{OM} . From the left to the right in Fig. 2, z values are increased by 1–2 times as ζ_{OM} increases, which can be expected from Eq. (7); while from the top to the bottom, z values are increased by more than one order of magnitude when the ambient temperature increases by 21 K. Thus, for docosane, the calculation of z value (or S value) is more sensitive to the changes in ambient temperature than the prescribed changes in activity coefficient. This is largely due to the exponential increase in vapor pressure with temperature of docosane and other SVOCs (Eq. 3).

Within each mesh plot, z value has a linear and reciprocal relationship with \overline{MW}_{OM} and M_{OM} , respectively, which can also be expected from Eq. (7). The maximum z value is 7.4 times as the minimum z value in each mesh plot. In this test, the variations of \overline{MW}_{OM} is much larger than that of M_{OM} , so the effects of \overline{MW}_{OM} to the calculation of z value seems more important than that of OM/OC ratio. However, if M_{OM} and \overline{MW}_{OM} have similar variations (e.g. OM/OC ranges from 1.2 to 2.0, and \overline{MW}_{OM} ranges from 150 to 250 g mol⁻¹), then these two parameters should have similar effects on the calculation of z value (or S value).

As demonstrated by the sensitivity study, the estimation of total SVOC concentration is mostly sensitive to ambient temperature. In this work, the sensitivity of G/P partitioning to ambient temperature is largely accounted for by adjusting the vapor pressure of each SVOC according to the daily average temperature. However, the total SVOC concentration estimated in the current work might be subject to considerable uncertainty due to the variations of ζ_{OM} , \overline{MW}_{OM} and OM/OC ratio across the sampling period.

3.3 PMF results for the full data set

A 7-factor solution was determined for the full data set using total SVOC concentration due to the most readily interpretable resulting factors and a relatively high factor matching rate of 79.9% between bootstrapped and base case solutions (Table 2). These seven factors are identified as nitrate, sulfate, n -alkane, sterane, light SVOC, PAH and bulk carbon. Figures S1 and S2 present the median factor profiles and contributions

with one standard deviation from bootstrapped PMF solutions, which represent the variability of PMF solution due to random sampling error. The factor contributions are also summarized by day of the week in boxplots (Fig. S3). The factor profiles have been normalized by

$$F_{kj}^* = \frac{F_{kj}}{\sum_{k=1}^p F_{kj}} \quad (8)$$

where F_{kj}^* is the relative weighting of species j in factor k to all other factors. The median factor contributions in Fig. S2 are expressed as reconstructed $\text{PM}_{2.5}$ mass – the sum of nitrate, sulfate, EC and straight OC fractions contributed by each factor. The contribution time series were divided into three periods (cold, warm and hot) and shown as the average contributions to major $\text{PM}_{2.5}$ components (nitrate, sulfate, EC and OC; Table 3). The sum of factor contributions to each component can be compared with the observed average concentration (Table 3). The sampling variability of factor contributions are represented by the median CVs (CV = standard deviation/median factor contribution). In addition, the factor contributions during each period were linearly regressed to meteorological and trace gas measurements in the same manner as discussed in the previous Xie et al. (2013) study, so as to understand the association between each factor and pollution sources/processes. The resulting correlation coefficients are given in Table S6.

In Table 3, the nitrate and sulfate concentrations are dominated by the nitrate (average 59.4%–97.4%) and sulfate (79.5%–96.0%) factors in all periods. In cold periods, the PAH factor (39.9%) had the highest contribution to EC concentrations, followed by the sterane (25.2%) and bulk carbon (23.0%) factors; while in warm and hot periods, the bulk carbon factor contributed the most of the EC concentrations (warm, 53.3%; hot, 76.5%). The bulk carbon factor also has the highest contribution to OC (36.6%–67.9%) in all periods. Here the OC consists of the three less or non-volatile OC fractions (OC2, OC3 and PC) that were used for source apportionment. The factors with small contributions to reconstructed $\text{PM}_{2.5}$ are prone to having high variability, as

Positive matrix factorization of $\text{PM}_{2.5}$

M. Xie et al.

Title Page

Abstract

Introduction

Conclusions

References

Tables

Figures

◀

▶

◀

▶

Back

Close

Full Screen / Esc

Printer-friendly Version

Interactive Discussion



shown by their higher CVs (e.g. *n*-alkane, sterane and PAH factors). In each period, the sum of factor contributions to each major PM_{2.5} component is close to the observed average concentration.

3.4 Comparison to filter-based source apportionment

In the previous Xie et al. (2013) study, an 8-factor solution was determined with factors labeled as inorganic ion, *n*-alkanes, EC/sterane, light *n*-alkane/PAH, medium alkane/alkanoic acid, PAH, winter/methoxyphenol and summer/odd *n*-alkane. The medium alkane/alkanoic acid and winter/methoxyphenol factors only contributed a small part (0.41%–1.10%; 0.16%–4.21%) of reconstructed PM_{2.5} mass and were not resolved in this study. The 7 factors resolved in the current work could be matched with the remaining 6 factors in the filter-based solution after combining the nitrate and sulfate factors. Correlations of factor contributions between the matched pairs of factors are shown in Fig. 3.

The factors characterized by inorganic ions, heavy *n*-alkanes and steranes exhibit strong correlations ($r = 0.92$ – 0.98) between the filter-based and total SVOC-based PMF solutions (Fig. 3). This strong correlation is because these factors are primarily linked with secondary formation or primary emission, and the heavy *n*-alkanes and steranes are mostly distributed in particle phase (Fig. 1). The light *n*-alkane/PAH and PAH factors from the filter-based solution are less correlated with the light SVOC ($r = 0.73$) and PAH ($r = 0.84$) factors from the total SVOC-based solution (Fig. 3). This is because these factors contain a significant fraction of light organic compounds, being subject more strongly to G/P partitioning. In Fig. 4a, the light SVOC factor shows an increase in contribution when the temperature rises, supporting the association of this factor with fossil fuel evaporation and biogenic emissions. In contrast, the light *n*-alkane/PAH factor from the filter-based solution exhibits low contributions in mid-summer when the temperature is the highest of the year and small peaks in winter when the temperature is low (Fig. 4b). The high temperatures in mid-summer keep light organic compounds in the gas phase, while the low temperatures in winter benefit

Positive matrix factorization of PM_{2.5}

M. Xie et al.

Title Page

Abstract

Introduction

Conclusions

References

Tables

Figures

◀

▶

◀

▶

Back

Close

Full Screen / Esc

Printer-friendly Version

Interactive Discussion



Positive matrix factorization of PM_{2.5}

M. Xie et al.

Title Page

Abstract

Introduction

Conclusions

References

Tables

Figures

◀

▶

◀

▶

Back

Close

Full Screen / Esc

Printer-friendly Version

Interactive Discussion



the partitioning of gas-phase organics to the particle phase. In addition, the high ozone concentrations in mid-summer could also be responsible for the decrease in factor contribution, since negative correlations have been observed between ozone concentration and the two matched factors (Light SVOC: -0.48 , Table S6; light n -alkane/PAH: -0.52 , Xie et al., 2013) from both solutions during hot periods. No obvious difference in contribution time series was observed for the PAH factor between the filter-based and total SVOC-based PMF solutions, since the PAH factor was mostly characterized by medium and high MW PAHs ($MW \geq 226$; Fig. S1f).

The bulk carbon factor in the current work contains the largest percentages of EC and OC fractions (Fig. S1g), and has maximum contributions in summer (Fig. S2g). This factor should be influenced by both secondary organic aerosols (SOA), as supported by the correlation between the factor contribution and ozone concentrations in hot periods ($r = 0.36$; Table S6), and primary emissions from motor vehicles, as supported by the weekend decrease in factor contribution (Fig. S3g) and the correlations between the factor contribution and NO_x and CO concentrations (Table S6). The summer/odd n -alkane factor from the filter-based solution was primarily associated with SOA formation, which lead to a moderate correlation ($r = 0.69$; Fig. 3f) with the bulk carbon factor in the current work. Except the inorganic ion factors, all other carbonaceous factors from the filter-based solution show higher contributions than their matched factors from the total SVOC-based solution, as illustrated by the regression slopes ranging from 1.3 to 2.7 (Fig. 3). This can mostly be attributed to the fact that the OC1 fraction was not included for source apportionment in the current study, which accounted for 47.6 % of the total OC on average.

3.5 PMF results for temperature-stratified sub-data sets

Statistics of PMF simulations for the three temperature-stratified sub-data sets are given in Table 2. Comparing to the full data set, the same species and factor number were chosen for PMF analysis of the cold and warm period sub-data sets. The factor matching rates are 88.6 % and 77.2 %, respectively (Table 2). For the hot period

Positive matrix factorization of PM_{2.5}

M. Xie et al.

Title Page

Abstract

Introduction

Conclusions

References

Tables

Figures

◀

▶

◀

▶

Back

Close

Full Screen / Esc

Printer-friendly Version

Interactive Discussion



sub-data set, fewer species were used to obtain physically meaningful solution with high factor matching rate. Finally, a 7-factor solution was chosen with a factor matching rate of 61.9 % (Table 2). Figures S4–S6 show the normalized factor profiles for each sub-data set solution with one standard deviation. The median factor contributions to major PM_{2.5} components during each period were averaged and presented in Table 3, and can be compared to those from full data set solution. Median CVs of factor contributions are also included in Table 3 to reflect the variability from random sampling error. In addition, the correlations between factor contributions and meteorological and trace gas measurements are given in Table S7. Similarly to the full data set solution, the nitrate and sulfate concentrations are mostly accounted for by the nitrate (average 93.9 %–94.7 %) and sulfate (85.2 %–87.9 %) factors (Table 3). The EC and OC concentrations are highest apportioned to the bulk carbon factor (EC, 48.9 %–64.9 %; OC, 32.9 %–50.7 %) for all periods.

3.6 Comparison to PMF results of the full data set

The factors from the analysis of each temperature-stratified sub-data set were matched to those from the full data set based on factor profiles. The linear regressions of factor contributions between matched pairs of factors are given in Table 4, so as to verify that the influence of G/P partitioning was eliminated from the PMF analysis by using the total SVOC data set. However, we cannot rule out the impacts of other atmospheric processes like photochemical reactions.

3.6.1 Cold period

All the factors resolved by using the cold period sub-data set show similar factor profiles as their corresponding factors from the full data set solution (Figs. S1 and S4). The EC concentration is more strongly apportioned to the bulk carbon factor from the cold period solution (average 63.8 %) than that from the full data set solution (22.2 %; Table 3). Moreover, strong correlations were observed between the bulk carbon factor

Positive matrix factorization of PM_{2.5}

M. Xie et al.

[Title Page](#)[Abstract](#)[Introduction](#)[Conclusions](#)[References](#)[Tables](#)[Figures](#)[◀](#)[▶](#)[◀](#)[▶](#)[Back](#)[Close](#)[Full Screen / Esc](#)[Printer-friendly Version](#)[Interactive Discussion](#)

from the cold period solution and NO_x ($r = 0.76$) and CO ($r = 0.76$; Table S7) concentrations. As such, the bulk carbon factor from the cold period solution should be mainly associated with primary emissions (e.g. gasoline and diesel vehicles). The full data set solution assumes constant co-influence of primary and secondary sources throughout the sampling period, which leads to a moderate correlation ($r = 0.54$; Table 4) of the bulk carbon factor between the full data set and cold period solutions. For other factors, relatively strong correlations ($r = 0.96$ – 1.00 ; Table 4) were observed between the two solutions, indicating that these matched pairs of factors could be linked to similar pollution sources/processes. Among all the factors, the light SVOC factor is most likely influenced by G/P partitioning when we only use the filter measurement data for source apportionment. The influence of G/P partitioning should be different across different periods due to the distinct temperature ranges, while the filter-based full data set solution assumes constant G/P partitioning influence. In Fig. 5a, d, the light *n*-alkane/PAH factor from the filter-based PMF analysis was more poorly correlated ($r = 0.41$) between the cold period and the full data set solutions (Xie et al., 2013) than the light SVOC factor from the total SVOC-based PMF analysis ($r = 0.96$). These results suggested that the G/P partitioning influence was removed from PMF analysis by using the total SVOC data set as input.

3.6.2 Warm period

The factors resolved by using the warm period sub-data set are also similar as those from the full data set solution on factor profiles (Figs. S1 and S5). Moreover, the factor contributions of the warm period and full data set solutions are relatively strongly correlated ($r = 0.96$ – 0.99) with regression slopes close to unity (0.73 – 1.30 ; Table 4). Such consistency between the warm period and full data set solutions was also observed in the previous Xie et al. (2013) study. One explanation is that the PMF model is solved by minimizing the sum of the squared, scaled residues, and then requires the mean concentrations of most species to be fit well. The average concentrations of most SVOCs in warm periods are closer to the averages of the whole period than those during cold

and hot periods. Thus, the factor contributions of the warm period solution are more consistent with those of the full data set solution.

3.6.3 Hot period

For the hot period, the nitrate measurements were not included for source apportionment due to the high percentages of missing and BDL observations, resulting in the omission of the nitrate factor. Meanwhile, a new factor was resolved and labeled as median *n*-alkane. It contains significant fraction of *n*-alkane with a chain length ranging from 22 to 29 (Fig. S6g). The factor contribution was moderately correlated with ambient temperature ($r = 0.59$) and anti-correlated with relative humidity ($r = -0.45$; Table S7). So the median *n*-alkane factor might be linked with temperature-dependent summertime emissions with contribution time series opposing to that of relative humidity. The median *n*-alkane factor was also identified by using the filter-based sub-data set for hot periods (Xie et al., 2013), and well correlated ($r = 0.80$) with that identified in this work. The other factors were matched to those from the full data set solution with strong correlations ($r = 0.79-0.99$; Table 4). However, the regression plot for the light SVOC factor in hot periods (Fig. 5f) is more scattered than those in cold and warm periods (Fig. 5d, e); and from the cold to hot periods, the light SVOC factor becomes less correlated with ambient temperature ($r, 0.61 \rightarrow 0.07$; Table S7). These could be caused by the increased photochemical reactions during hot periods, supported by the negative correlation ($r = -0.46$) between the light SVOC factor and ozone concentration.

4 Conclusions

The gas-phase concentrations of 71 SVOCs were estimated using particle-phase measurements by G/P partitioning theory. In order to eliminate the impacts of G/P partitioning on PMF analysis, the gas-phase concentrations of all SVOCs were added to their

Positive matrix factorization of PM_{2.5}

M. Xie et al.

Title Page

Abstract

Introduction

Conclusions

References

Tables

Figures

◀

▶

◀

▶

Back

Close

Full Screen / Esc

Printer-friendly Version

Interactive Discussion



Positive matrix factorization of PM_{2.5}

M. Xie et al.

Title Page

Abstract

Introduction

Conclusions

References

Tables

Figures

◀

▶

◀

▶

Back

Close

Full Screen / Esc

Printer-friendly Version

Interactive Discussion



particle-phase concentrations as inputs for source apportionment. Seven factors were identified from the full data set, including the nitrate, sulfate, *n*-alkane, sterane, light SVOC, PAH and bulk carbon factors, and could be matched to those from a previous filter-based PMF study (Xie et al., 2013) with reasonable ($r = 0.69$) to excellent ($r = 0.98$) correlations. Three temperature-stratified sub-data sets, representing ambient sampling during the cold, warm and hot periods, were also analyzed using PMF. Unlike the light *n*-alkane/PAH factor from the filter-based study, the light SVOC factor from the total-SVOC based PMF solution exhibited strong correlations ($r = 0.82$ – 0.98) between the full data set and each sub-data set solutions. These results suggested that the influences of G/P partitioning on PMF analysis could be removed by using total SVOC (gas + particle phase) data. However, the impact of photochemical process has not been ruled out in this work, as illustrated by the moderate correlation ($r = 0.54$) between the bulk carbon factor of the full data set solution and that of the cold period solution.

This study is our first step in improving SVOC-based PMF analysis by removing the impacts of G/P partitioning. However, the pre-assumptions (e.g. MW_{OM} and ζ_{OM} values) made for the calculation of gas-phase SVOC concentrations need to be verified, and if necessary refined, by comparing with field measurements. Additionally, more source markers are required to further apportion the bulk carbon factor. Finally, gas-phase OC data are needed to further understand the ambient OC sources. All of the above will be considered in our subsequent work.

Supplementary material related to this article is available online at:

<http://www.atmos-chem-phys-discuss.net/13/5199/2013/acpd-13-5199-2013-supplement.pdf>.

Disclaimer. The views expressed are those of the authors and do not necessarily reflect the views or policies of the US Environmental Protection Agency.

Acknowledgements. This research is supported by NIEHS research grant number RO1 ES010197.

References

- 5 Bae, M. S., Demerjian, K. L., and Schwab, J. J.: Seasonal estimation of organic mass to organic carbon in PM_{2.5} at rural and urban locations in New York state, *Atmos. Environ.*, 40, 7467–7479, 2006.
- Barsanti, K. C. and Pankow, J. F.: Thermodynamics of the formation of atmospheric organic particulate matter by accretion reactions – Part 1: aldehydes and ketones, *Atmos. Environ.*, 38, 4371–4382, 2004.
- 10 Chang, E. I. and Pankow, J. F.: Organic particulate matter formation at varying relative humidity using surrogate secondary and primary organic compounds with activity corrections in the condensed phase obtained using a method based on the Wilson equation, *Atmos. Chem. Phys.*, 10, 5475–5490, doi:10.5194/acp-10-5475-2010, 2010.
- Chen, L. W. A., Watson, J. G., Chow, J. C., DuBois, D. W., and Herschberger, L.: PM_{2.5} source apportionment: reconciling receptor models for US nonurban and urban long-term networks, *J. Air Waste Manage.*, 61, 1204–1217, 2011.
- 15 Dutton, S. J., Schauer, J. J., Vedal, S., and Hannigan, M. P.: PM_{2.5} characterization for time series studies: pointwise uncertainty estimation and bulk speciation methods applied in Denver, *Atmos. Environ.*, 43, 1136–1146, 2009a.
- 20 Dutton, S. J., Williams, D. E., Garcia, J. K., Vedal, S., and Hannigan, M. P.: PM_{2.5} characterization for time series studies: organic molecular marker speciation methods and observations from daily measurements in Denver, *Atmos. Environ.*, 43, 2018–2030, 2009b.
- Dutton, S. J., Vedal, S., Piedrahita, R., Milford, J. B., Miller, S. L., and Hannigan, M. P.: Source apportionment using positive matrix factorization on daily measurements of inorganic and organic speciated PM_{2.5}, *Atmos. Environ.*, 44, 2731–2741, 2010.
- 25 Fraser, M. P., Cass, G. R., Simoneit, B. R. T., and Rasmussen, R. A.: Air quality model evaluation data for organics, Part 4: C₂–C₃₆ non-aromatic hydrocarbons, *Environ. Sci. Technol.*, 31, 2356–2367, 1997.

Positive matrix factorization of PM_{2.5}

M. Xie et al.

Title Page

Abstract

Introduction

Conclusions

References

Tables

Figures

◀

▶

◀

▶

Back

Close

Full Screen / Esc

Printer-friendly Version

Interactive Discussion



Positive matrix factorization of PM_{2.5}

M. Xie et al.

[Title Page](#)[Abstract](#)[Introduction](#)[Conclusions](#)[References](#)[Tables](#)[Figures](#)[◀](#)[▶](#)[◀](#)[▶](#)[Back](#)[Close](#)[Full Screen / Esc](#)[Printer-friendly Version](#)[Interactive Discussion](#)

Fraser, M. P., Cass, G. R., Simoneit, B. R. T., and Rasmussen, R. A.: Air quality model evaluation data for organics, Part 5: C₆–C₂₂ nonpolar and semipolar aromatic compounds, *Environ. Sci. Technol.*, 32, 1760–1770, 1998.

Hallquist, M., Wenger, J. C., Baltensperger, U., Rudich, Y., Simpson, D., Claeys, M., Dommen, J., Donahue, N. M., George, C., Goldstein, A. H., Hamilton, J. F., Herrmann, H., Hoffmann, T., Iinuma, Y., Jang, M., Jenkin, M. E., Jimenez, J. L., Kiendler-Scharr, A., Maenhaut, W., McFiggans, G., Mentel, Th. F., Monod, A., Prévôt, A. S. H., Seinfeld, J. H., Surratt, J. D., Szmigielski, R., and Wildt, J.: The formation, properties and impact of secondary organic aerosol: current and emerging issues, *Atmos. Chem. Phys.*, 9, 5155–5236, doi:10.5194/acp-9-5155-2009, 2009.

Hemann, J. G., Brinkman, G. L., Dutton, S. J., Hannigan, M. P., Milford, J. B., and Miller, S. L.: Assessing positive matrix factorization model fit: a new method to estimate uncertainty and bias in factor contributions at the measurement time scale, *Atmos. Chem. Phys.*, 9, 497–513, doi:10.5194/acp-9-497-2009, 2009.

Hilal, S. H., Karickhoff, S. W., and Carreira, L. A.: A rigorous test for SPARC's chemical reactivity models: estimation of more than 4300 ionization pK_a s, *Quant. Struct.-Act. Rel.*, 14, 348–355, 1995.

Ito, K., Christensen, W. F., Eatough, D. J., Henry, R. C., Kim, E., Laden, F., Lall, R., Larson, T. V., Neas, L., Hopke, P. K., and Thurston, G. D.: PM source apportionment and health effects: 2. an investigation of inter-method variability in associations between source-apportioned fine particle mass and daily mortality in Washington, DC, *J. Expo. Sci. Env. Epid.*, 16, 300–310, 2006.

Jaekels, J. M., Bae, M. S., and Schauer, J. J.: Positive matrix factorization (PMF) analysis of molecular marker measurements to quantify the sources of organic aerosols, *Environ. Sci. Technol.*, 41, 5763–5769, 2007.

Kim, S.-Y., Peel, J. L., Hannigan, M. P., Dutton, S. J., Sheppard, L., Clark, M. L., and Vedal, S.: The temporal lag structure of short-term associations of fine particulate matter chemical constituents and cardiovascular and respiratory hospitalizations, *Environ. Health Persp.*, 120, 1094–1099, 2012.

Laden, F., Neas, L. M., Dockery, D. W., and Schwartz, J.: Association of fine particulate matter from different sources with daily mortality in six US Cities, *Environ. Health Persp.*, 108, 941–947, 2000.

Positive matrix factorization of PM_{2.5}

M. Xie et al.

Title Page

Abstract

Introduction

Conclusions

References

Tables

Figures

◀

▶

◀

▶

Back

Close

Full Screen / Esc

Printer-friendly Version

Interactive Discussion



- Liang, C. and Pankow, J. F.: Gas/particle partitioning of organic compounds to environmental tobacco smoke: partition coefficient measurements by desorption and comparison to urban particulate material, *Environ. Sci. Technol.*, 30, 2800–2805, 1996.
- Liang, C., Pankow, J. F., Odum, J. R., and Seinfeld, J. H.: Gas/particle partitioning of semivolatile organic compounds to model inorganic, organic, and ambient smog aerosols, *Environ. Sci. Technol.*, 31, 3086–3092, 1997.
- Mader, B. T. and Pankow, J. F.: Study of the effects of particle-phase carbon on the gas/particle partitioning of semivolatile organic compounds in the atmosphere using controlled field experiments, *Environ. Sci. Technol.*, 36, 5218–5228, 2002.
- Mandalakis, M., Tzapakis, M., Tsoga, A., and Stephanou, E. G.: Gas–particle concentrations and distribution of aliphatic hydrocarbons, PAHs, PCBs and PCDD/Fs in the atmosphere of Athens (Greece), *Atmos. Environ.*, 36, 4023–4035, 2002.
- Mar, T. F., Ito, K., Koenig, J. Q., Larson, T. V., Eatough, D. J., Henry, R. C., Kim, E., Laden, F., Lall, R., Neas, L., Stolzel, M., Paatero, P., Hopke, P. K., and Thurston, G. D.: PM source apportionment and health effects, Part 3: investigation of inter-method variations in associations between estimated source contributions of PM_{2.5} and daily mortality in Phoenix, AZ, *J. Expo. Sci. Env. Epid.*, 16, 311–320, 2005.
- May, A. A., Saleh, R., Hennigan, C. J., Donahue, N. M., and Robinson, A. L.: Volatility of organic molecular markers used for source apportionment analysis: measurements and atmospheric implications, *Environ. Sci. Technol.*, 46, 12435–12444, 2012.
- Nahir, T. M.: Analysis of semivolatile organic compounds in fuels using gas chromatography–mass spectrometry, *J. Chem. Educ.*, 76, 1695–1696, 1999.
- NIOSH: Method 5040, Issue 3: Diesel particulate matter (as elemental carbon), in: NIOSH Manual of Analytical Methods (NMAM), 4. edn., National Institute of Occupational Safety and Health, Cincinnati, OH, 1–5, 2003.
- Odum, J. R., Hoffmann, T., Bowman, F., Collins, D., Flagan, R. C., and Seinfeld, J. H.: Gas/particle partitioning and secondary organic aerosol yields, *Environ. Sci. Technol.*, 30, 2580–2585, 1996.
- Paatero, P.: User's Guide for Positive Matrix Factorization Program PMF2 and PMF3, Part 1: Tutorial, University of Helsinki, Helsinki, Finland, 1998a.
- Paatero, P.: User's Guide for Positive Matrix Factorization Program PMF2 and PMF3, Part 2: Reference, University of Helsinki, Helsinki, Finland, 1998b.

Positive matrix factorization of PM_{2.5}

M. Xie et al.

Title Page

Abstract

Introduction

Conclusions

References

Tables

Figures

◀

▶

◀

▶

Back

Close

Full Screen / Esc

Printer-friendly Version

Interactive Discussion



- Pankow, J. F.: An absorption model of gas/particle partitioning of organic compounds in the atmosphere, *Atmos. Environ.*, 28, 185–188, 1994a.
- Pankow, J. F.: An absorption model of the gas/aerosol partitioning involved in the formation of secondary organic aerosol, *Atmos. Environ.*, 28, 189–193, 1994b.
- 5 Pankow, J. F. and Asher, W. E.: SIMPOL.1: a simple group contribution method for predicting vapor pressures and enthalpies of vaporization of multifunctional organic compounds, *Atmos. Chem. Phys.*, 8, 2773–2796, doi:10.5194/acp-8-2773-2008, 2008.
- Pankow, J. F. and Chang, E. I.: Variation in the sensitivity of predicted levels of atmospheric organic particulate matter (OPM), *Environ. Sci. Technol.*, 42, 7321–7329, 2008.
- 10 Pun, B. K.: Development and initial application of the sesquiversion of MADRID, *J. Geophys. Res.*, 113, D12212, doi:10.1029/2008JD009888, 2008.
- Schauer, J. J., Mader, B. T., Deminter, J. T., Heidemann, G., Bae, M. S., Seinfeld, J. H., Flanagan, R. C., Cary, R. A., Smith, D., Huebert, B. J., Bertram, T., Howell, S., Kline, J. T., Quinn, P., Bates, T., Turpin, B., Lim, H. J., Yu, J. Z., Yang, H., and Keywood, M. D.: ACE-Asia inter-comparison of a thermal-optical method for the determination of particle-phase organic and elemental carbon, *Environ. Sci. Technol.*, 37, 993–1001, 2003.
- 15 Schnelle-Kreis, J., Sklorz, M., Orasche, J., Stölzel, M., Peters, A., and Zimmermann, R.: Semi-volatile organic compounds in ambient PM_{2.5}. Seasonal trends and daily resolved source contributions, *Environ. Sci. Technol.*, 41, 3821–3828, 2007.
- 20 Shrivastava, M. K., Subramanian, R., Rogge, W. F., and Robinson, A. L.: Sources of organic aerosol: positive matrix factorization of molecular marker data and comparison of results from different source apportionment models, *Atmos. Environ.*, 41, 9353–9369, 2007.
- Simcik, M. F., Zhang, H., Eisenreich, S. J., and Franz, T. P.: Urban contamination of the Chicago/coastal lake Michigan atmosphere by PCBs and PAHs during AEOLOS, *Environ. Sci. Technol.*, 31, 2141–2147, 1997.
- 25 Simcik, M. F., Franz, T. P., Zhang, H., and Eisenreich, S. J.: Gas-particle partitioning of PCBs and PAHs in the Chicago urban and adjacent coastal atmosphere: states of equilibrium, *Environ. Sci. Technol.*, 32, 251–257, 1998.
- Tsapakis, M. and Stephanou, E. G.: Occurrence of gaseous and particulate polycyclic aromatic hydrocarbons in the urban atmosphere: study of sources and ambient temperature effect on the gas/particle concentration and distribution, *Environ. Pollut.*, 133, 147–156, 2005.
- 30

Positive matrix factorization of PM_{2.5}

M. Xie et al.

[Title Page](#)[Abstract](#)[Introduction](#)[Conclusions](#)[References](#)[Tables](#)[Figures](#)[I◀](#)[▶I](#)[◀](#)[▶](#)[Back](#)[Close](#)[Full Screen / Esc](#)[Printer-friendly Version](#)[Interactive Discussion](#)

- Vedal, S., Hannigan, M. P., Dutton, S. J., Miller, S. L., Milford, J. B., Rabinovitch, N., Kim, S. Y., and Sheppard, L.: The denver aerosol sources and health (DASH) study: overview and early findings, *Atmos. Environ.*, 43, 1666–1673, 2009.
- Williams, B. J., Goldstein, A. H., Kreisberg, N. M., and Hering, S. V.: In situ measurements of gas/particle-phase transitions for atmospheric semivolatile organic compounds, *P. Natl. Acad. Sci. USA*, 107, 6676–6681, 2010.
- 5 Xie, M., Piedrahita, R., Dutton, S. J., Milford, J. B., Hemann, J. G., Peel, J. L., Miller, S. L., Kim, S.-Y., Vedal, S., Sheppard, L., and Hannigan, M. P.: Positive matrix factorization of a 32-month series of daily PM_{2.5} speciation data with incorporation of temperature stratification,
- 10 *Atmos. Environ.*, 65, 11–20, 2013.

Positive matrix factorization of PM_{2.5}

M. Xie et al.

Title Page

Abstract

Introduction

Conclusions

References

Tables

Figures

◀

▶

◀

▶

Back

Close

Full Screen / Esc

Printer-friendly Version

Interactive Discussion

**Table 1.** Values of parameters used to test the sensitivity of total SVOC estimation.

Parameters	Cold	Warm	Hot
T (K)	276.5	288.5	297.6
M_{oc} ($\mu\text{g m}^{-3}$) ^a	2.78	2.39	3.45
p_L^o (atm) ^b	8.52×10^{-10}	6.80×10^{-9}	2.96×10^{-8}
ζ_{OM}		0.5, 1, 1.5	
MW_{OM} (g mol^{-1}) ^c		50, 150, 200, 30	
OM/OC		1.3, 1.4, 1.5, 1.6	

^a Mean organic carbon concentrations during different periods.^b Vapor pressures of docosane at different temperatures.^c Mean molecular weight of absorbing organic material.

Positive matrix factorization of PM_{2.5}

M. Xie et al.

Title Page

Abstract

Introduction

Conclusions

References

Tables

Figures

◀

▶

◀

▶

Back

Close

Full Screen / Esc

Printer-friendly Version

Interactive Discussion



Table 2. PMF simulation statistics for different data sets.

Parameters	Data sets			
	Full	Cold	Warm	Hot
No. of species	52	52	52	37
No. of samples	970	364	318	288
No. of factors	7	7	7	7
No. of bootstrap replicate data sets	1000	1000	1000	1000
No. of data sets for which PMF did not converge to a solution	0	0	0	0
No. of data sets for which factors were uniquely matched	799	886	772	619

Table 3. Average factor contributions to bulk components for full data set solution and sub-data set solutions ($\mu\text{g m}^{-3}$).

Factors	Full data set solution					Sub-data set solution				
	Nitrate	Sulfate	EC	OC ^a	CV ^b	Nitrate	Sulfate	EC	OC	CV
	Cold period					Cold period				
Nitrate	2.2	0.24	0.060	0.076	0.036	2.1	0.14	0.031	0.14	0.074
Sulfate	0.035	1.0	0.0026	0.022	0.060	0.12	1.1	0.015	0.015	0.11
<i>n</i> -Alkane	0.0004	0.0079	0.0003	0.26	0.35	0.0007	0.0023	0.00	0.25	0.27
Sterane	0.0008	0.0079	0.13	0.17	0.52	0.012	0.023	0.070	0.10	0.52
Light SVOC	0.0009	0.0013	0.0012	0.027	0.22	0.0040	0.0045	0.030	0.18	0.14
PAH	0.0003	0.0010	0.21	0.15	0.31	0.0005	0.0030	0.057	0.019	0.84
Bulk carbon	0.0081	0.0052	0.12	0.41	0.33	0.0009	0.0095	0.37	0.47	0.23
Subtotal	2.2	1.3	0.54	1.1		2.2	1.3	0.58	1.2	
Observed Conc.	2.2	1.3	0.61	1.4						
	Warm period					Warm period				
Nitrate	0.32	0.036	0.0089	0.011	0.23	0.37	0.10	0.028	0.021	0.44
Sulfate	0.032	0.93	0.0023	0.020	0.031	0.011	0.86	0.00	0.12	0.11
<i>n</i> -Alkane	0.0002	0.0038	0.0001	0.12	0.39	0.0026	0.0034	0.00	0.16	0.44
Sterane	0.0003	0.0031	0.053	0.069	0.61	0.0007	0.0090	0.069	0.068	0.68
Light SVOC	0.0041	0.0061	0.0056	0.12	0.15	0.0012	0.0069	0.012	0.14	0.15
PAH	0.0002	0.0005	0.11	0.082	0.33	0.0001	0.0003	0.091	0.057	0.41
Bulk carbon	0.014	0.0089	0.21	0.70	0.13	0.0050	0.0010	0.19	0.58	0.21
Subtotal	0.37	0.99	0.39	1.1		0.39	0.98	0.39	1.1	
Observed Conc.	0.40	1.0	0.43	1.2						
	Hot period					Hot period				
Nitrate	0.11	0.012	0.0030	0.0038	0.35	–	–	–	–	–
Sulfate	0.040	1.2	0.0029	0.025	0.037	–	1.0	0.035	0.13	0.14
<i>n</i> -Alkane	0.0002	0.0031	0.0001	0.10	0.46	–	0.0001	0.051	0.46	0.50
Sterane	0.0002	0.0020	0.035	0.045	0.73	–	0.035	0.077	0.24	0.52
Light SVOC	0.011	0.016	0.015	0.33	0.15	–	0.079	0.012	0.11	0.30
PAH	0.0001	0.0002	0.051	0.037	0.37	–	0.0005	0.039	0.0070	0.74
Bulk carbon	0.023	0.015	0.35	1.2	0.14	–	0.056	0.22	0.55	0.39
Median <i>n</i> -alkane	–	–	–	–	–	–	0.0026	0.0070	0.17	0.56
Subtotal	0.18	1.2	0.45	1.7		–	1.2	0.44	1.7	
Observed Conc.	0.19	1.2	0.46	1.8						

^a Sum of contributions to OC2, OC3 and PC fractions.

^b Median coefficient of variation (CV) of factor contributions, CV = standard deviation/median factor contribution.

Positive matrix factorization of PM_{2.5}

M. Xie et al.

Title Page

Abstract

Introduction

Conclusions

References

Tables

Figures

◀

▶

◀

▶

Back

Close

Full Screen / Esc

Printer-friendly Version

Interactive Discussion



Positive matrix factorization of PM_{2.5}

M. Xie et al.

Title Page

Abstract

Introduction

Conclusions

References

Tables

Figures

◀

▶

◀

▶

Back

Close

Full Screen / Esc

Printer-friendly Version

Interactive Discussion



Table 4. Regression statistics of factor contributions between full data set and sub-data set solutions.

Factor		Cold			Warm			Hot		
Full ^a	Sub ^b	Slope	Intercept	<i>r</i>	Slope	Intercept	<i>r</i>	Slope	Intercept	<i>r</i>
Nitrate	Nitrate	0.94	−49.7	1.00	1.20	56.7	0.98	−	−	−
Sulfate	Sulfate	1.12	33.2	1.00	1.02	−20.9	0.99	1.12	−219	0.99
<i>n</i> -alkane	<i>n</i> -alkane	0.98	−4.18	0.98	1.17	14.5	0.99	3.37	162	0.79
Sterane	Sterane	0.70	12.8	0.98	1.19	−2.65	0.99	3.45	71.8	0.81
Light SVOC	Light SVOC	5.34	50.2	0.96	1.30	−21.2	0.98	0.80	−102	0.82
PAH	PAH	0.24	−10.9	0.97	0.73	5.33	0.99	0.39	12.6	0.91
Bulk carbon	Bulk carbon	1.12	236	0.54	0.96	−118	0.96	0.59	−80.5	0.81
Sum ^c	Sum	1.02	−34.3	0.99	1.00	17.9	0.99	0.74	153	0.89

^a Full data set solution, of which the factor contribution were regarded as independent variables for regression.

^b Temperature-stratified sub-data set solutions.

^c Sum of factor contributions.

Positive matrix factorization of PM_{2.5}

M. Xie et al.

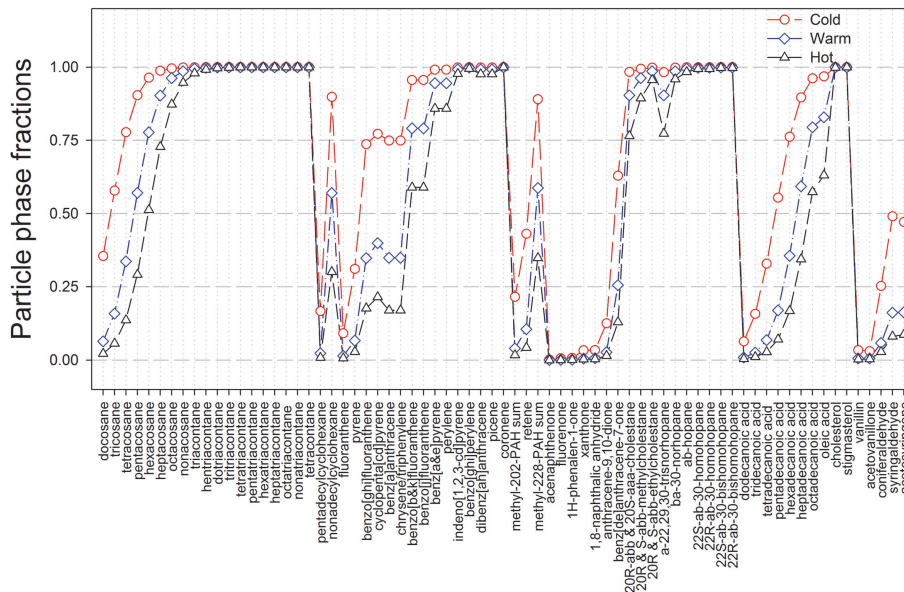


Fig. 1. Mean particle-phase fractions of all SVOCs during cold, warm and hot periods.

Title Page

Abstract Introduction

Conclusions References

Tables Figures

◀ ▶

◀ ▶

Back Close

Full Screen / Esc

Printer-friendly Version

Interactive Discussion



Title Page

Abstract

Introduction

Conclusions

References

Tables

Figures

◀

▶

◀

▶

Back

Close

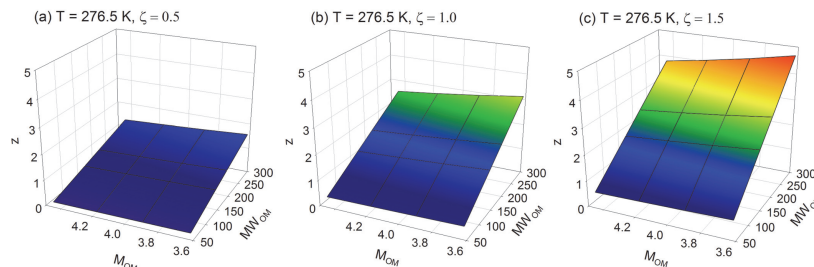
Full Screen / Esc

Printer-friendly Version

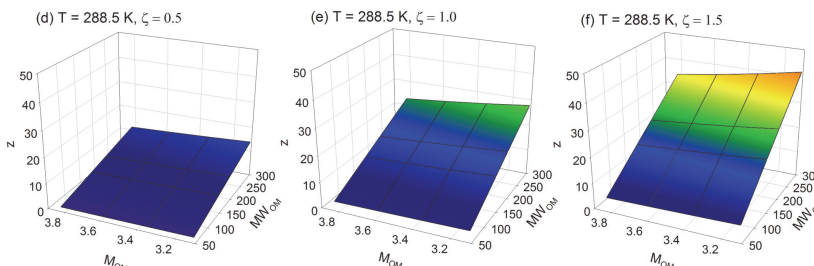
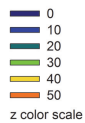
Interactive Discussion



Cold



Warm



Hot

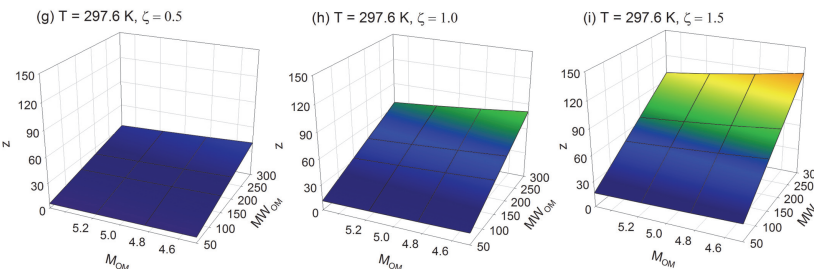
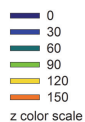


Fig. 2. Sensitivity of the calculation of total SVOC concentration (S value), determined by z value, to ambient temperature (T), mole fraction scale activity coefficient (ζ_{OM}), OM/OC ratio and mean molecular weight of absorbing OM phase (\overline{MW}_{OM}). The z value equals to the ratio of gas phase to particle phase SVOC.

Positive matrix factorization of PM_{2.5}

M. Xie et al.

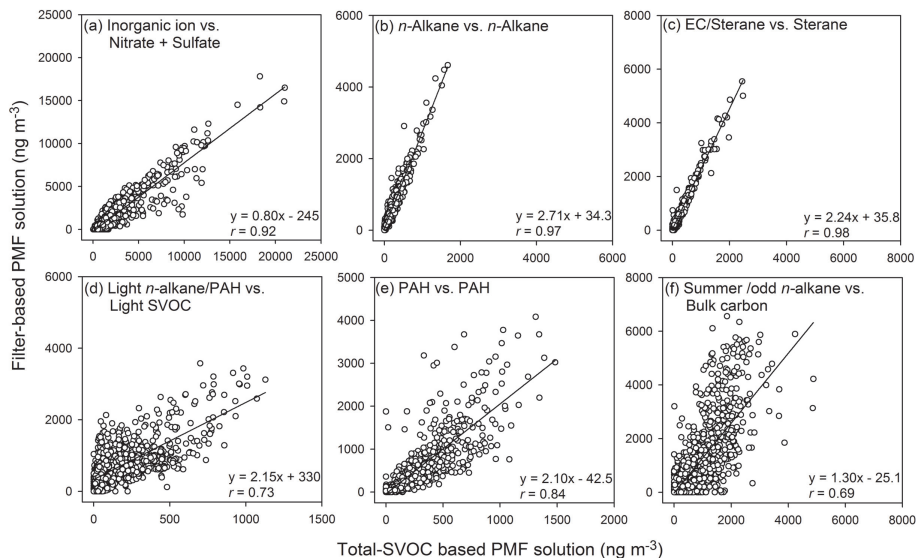


Fig. 3. Linear regressions of matched pairs of factors between filter-based and total SVOC-based PMF analysis.

Title Page

Abstract

Introduction

Conclusions

References

Tables

Figures

◀

▶

◀

▶

Back

Close

Full Screen / Esc

Printer-friendly Version

Interactive Discussion



Positive matrix factorization of PM_{2.5}

M. Xie et al.

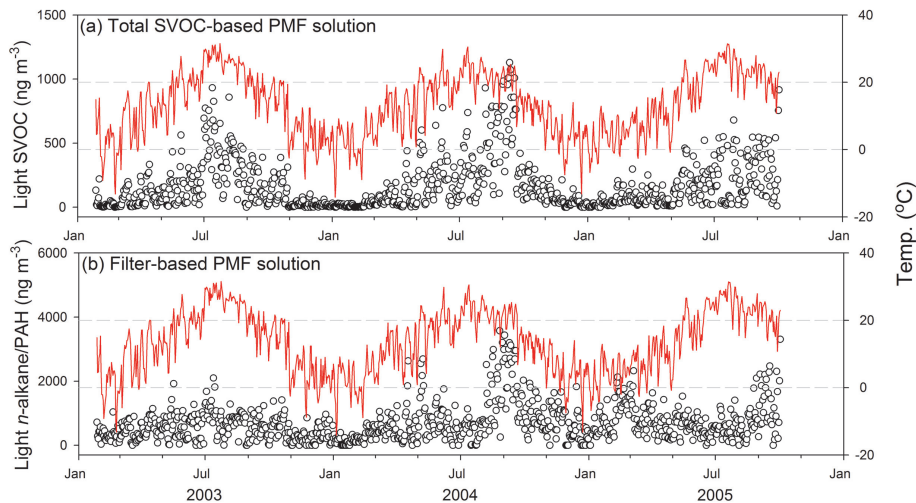


Fig. 4. Median factor contribution time series (blank circle) of **(a)** light SVOC factor from the total SVOC-based solution, and **(b)** light *n*-alkane/PAH factor from the filter-based solution. The red line represents the timeseries of daily average temperature.

[Title Page](#)[Abstract](#)[Introduction](#)[Conclusions](#)[References](#)[Tables](#)[Figures](#)[◀](#)[▶](#)[◀](#)[▶](#)[Back](#)[Close](#)[Full Screen / Esc](#)[Printer-friendly Version](#)[Interactive Discussion](#)

Positive matrix factorization of PM_{2.5}

M. Xie et al.

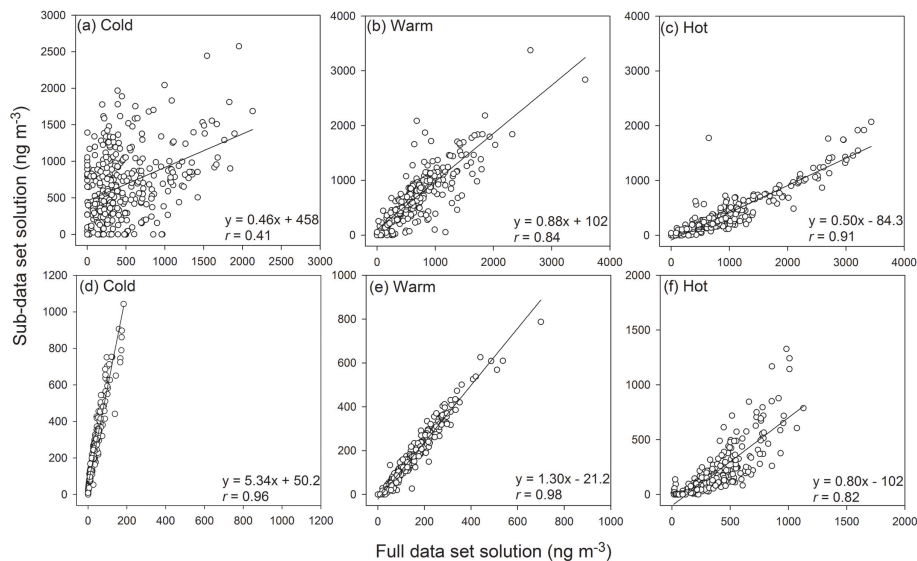


Fig. 5. Linear regressions of factor contributions between the full data set and sub-data set solutions, **(a–c)** light *n*-alkane/PAH factor from filter-based analysis; **(d–f)** light SVOC factor from total SVOC-based analysis.

[Title Page](#)[Abstract](#)[Introduction](#)[Conclusions](#)[References](#)[Tables](#)[Figures](#)[◀](#)[▶](#)[◀](#)[▶](#)[Back](#)[Close](#)[Full Screen / Esc](#)[Printer-friendly Version](#)[Interactive Discussion](#)